

## Numerical Heat Transfer and Pressure Drop Investigation of Different Height Baffles Mounted Simultaneously in a 2-D Channel

Mohamed Hamza<sup>1,3</sup>, Abdullatif A. Gari<sup>2</sup>

<sup>1</sup> Mechanical Engineering Department, Faculty of Engineering at Rabigh, King Abdulaziz University, Rabigh 21911, Saudi Arabia

<sup>2</sup> Mechanical Engineering Department, Engineering College at Jeddah, King Abdulaziz University, Jeddah 21589, Saudi Arabia

<sup>3</sup> Department of Mechanical Engineering, Faculty of Engineering, Assiut University, Assiut 71516, Egypt  
E-mail: [mohamedhamza010@gmail.com](mailto:mohamedhamza010@gmail.com), [agari@kau.edu.sa](mailto:agari@kau.edu.sa)

**ABSTRACT:** The objective of the current study is to numerically investigate the effect of different height baffles mounted simultaneously in a 2-dimensional channel on heat transfer and pressure drop. Three baffles of different height to channel ratios,  $e/H$ , of 0.167, 0.25, and 0.333, are used to form 9 different arrangements, or cases, of which seven cases have the same average baffle height,  $e/H$  of 0.167. Three of the 9 cases have equal height baffles. The Nusselt number ratio,  $Nu/Nu_s$ , and friction factor ratio,  $f/f_s$ , as functions of Reynolds number are to be studied. Two performance measures are applied, which are the standard deviation of temperature,  $\sigma_T$ , and the thermal performance enhancement factor,  $TEF$ . The results shows that  $Nu/Nu_s$ ,  $\sigma_T$ , and  $TEF$  decrease with Re. There is a proportional relationship between  $f/f_s$  and Re. Using a short baffle in front and a tall baffle in the back leads to decreasing the difference between the maximum and minimum temperatures of the heater plate, hence, decreasing the average  $\sigma_T$  values by up to 52%. Comparing the cases that have the same average baffle heights indicates that mounting tall baffles in front enhances  $Nu/Nu_s$  by 3%. For cases with equal average baffle heights, using baffles of equal height shows better performance from the  $TEF$  point of view.

[Mohamed Hamza, Abdullatif A. Gari. **Numerical Heat Transfer and Pressure Drop Investigation of Different Height Baffles Mounted Simultaneously in a 2-D Channel.** *Life Sci J* 2013;10(2):1711-1718].(ISSN:1097-8135). <http://www.lifesciencesite.com>. 241

**Keywords:** Numerical, turbulent flow, heat transfer, baffle, friction factor, Nusselt number

### 1. Introduction

Use of a baffle is one of the passive heat transfer augmentation techniques used in many industrial applications and devices, including solar collectors, internal cooling of turbine blades, cooling of electronics, and heat exchangers. Baffles enhance heat transfer by forming large-scale fluid bulk motion, but cause pressure drop increases due to the blockage of fluid flow. Some parameters that affect the heat transfer and pressure drop increase include: baffle blockage ratio ( $e/H$ ), pitch ratio ( $PR = P/H$ ), baffle orientation, baffle geometry and the Reynolds number.

Solid baffles staggered in a rectangular duct with different values of Reynolds numbers and baffle heights were studied by Habib et al. [1]. They found that as baffle height and the Reynolds number increased both, the heat transfer parameters and pressure loss increased. The increase of pressure loss was much higher than the heat transfer coefficient increase. Inclined solid and perforated baffles were investigated by Dutta and Hossain [2], who performed experimental investigations of two inclined solid and perforated baffles of the same overall size on the local heat transfer characteristics and the frictional head loss in a rectangular channel. The upstream baffle was attached to the top heated surface, while the position,

orientation, and the shape of the other baffle was varied to identify the optimum configuration for enhanced heat transfer. Experimental results showed that the local Nusselt number distribution was strongly dependent on the position, orientation, and geometry of the second baffle plate.

Karwa et al. [3] studied experimentally the heat transfer and friction in rectangular ducts with solid or perforated baffles attached to one of the broad walls. The baffle pitch-to-height ratio was 29 while the baffle height-to-duct height ratio was 0.495. It was found that the Nusselt number for the solid baffles was 73.7-82.7% higher than that for the smooth duct and the friction factor for the solid baffles was found to be 9.6-11.1 times greater than that of the smooth duct. Other experimental work on perforated baffles and porous baffles were conducted in [4], [5], [6], and [7].

Promvongse[8] conducted an experimental work to study the effect of 60° V-baffle turbulator on heat transfer and pressure drop. Three different baffles that had  $e/H$  values of 0.10, 0.20 and 0.30 and  $PR$  values of 1, 2 and 3 were studied at the Reynolds number value of 5,000 to 25,000. A maximum thermal enhancement factor of about 1.87 was achieved using the V-baffle with  $PR=1$  and  $e/H=0.10$  at the lower Reynolds number.

A numerical study of four inclined baffle types, one solid and three different perforated baffles, on the fluid flow and heat transfer in the rectangular channel was conducted by Oh et al. [9]. One baffle, with an inclination angle of  $5^\circ$ , was mounted on the rectangular channel. A 3-dimensional numerical simulation using the SST  $k - \omega$  turbulence model and more than 500,000 nodes were applied and the Reynolds number ranged between 23,000 and 57,000. The numerical results were compared with the experimental data. The discrepancies between the numerical results and the experimental data were attributed to different properties, buoyancy effects, and temperature measurement, which were done at the centerline while the numerical results were calculated over the entire domain.

Different types of perforated baffles with square diamond holes were investigated experimentally and numerically by Ary et al. [10]. The baffles had inclination angles of  $5^\circ$ . The results showed that the local heat transfer and the flow pattern were affected by the different number of holes. The heat transfer was greater when using two baffles compared with using a single baffle.

Kwankaomeng and Promvong [11], Promvong et al. [12], and Jedsadaratanachai et al. [13] conducted a numerical study on periodic laminar flow and heat transfer behaviors in a three-dimensional isothermal wall square duct fitted with  $30^\circ$  angled baffles on a lower duct wall and on two opposite walls respectively. Promvong et al. [14] conducted a numerical investigation of laminar periodic flow and heat transfer in a three-dimensional isothermal-wall square channel fitted with  $45^\circ$  inclined baffles. The  $45^\circ$  baffles generated a streamwise main vortex flow throughout the channel leading to a mixing of flow between the core and wall regions. Heat transfer rate also increased due to impingement jets induced by a longitudinal vortex pair of flow. The enhancement factor of the  $45^\circ$  baffle investigated was found to be higher than that of the  $90^\circ$  baffle for all Reynolds numbers and baffle heights. Another numerical study was conducted by Promvong et al. [15] using the  $45^\circ$  inclined baffles but mounted on two opposite walls. The  $45^\circ$  inline and staggered baffles show nearly the same results. The optimum thermal enhancement factor was at the  $45^\circ$  baffle height of 0.2 times greater than the channel height. Periodic laminar flow and heat transfer of a channel with  $45^\circ$  staggered solid V-baffles were investigated numerically by Promvong and Kwankaomeng [16]. The baffles were mounted staggered on the lower and upper walls of the channel. The V-baffle pointed upstream and on other runs downstream. The optimum thermal enhancement factor is higher for the V-baffle pointing downstream than upstream.

Z-shaped solid baffle turbulators have been experimentally and numerically studied by Sriromreun et al. [17]. The baffles were placed in a zigzag shape. The Reynolds number changed from 4400 to 20,400. Higher heat transfer and friction loss are achieved using larger  $e/H$  and shorter pitch length. The numerical model solved the Reynolds averaged Navier–Stokes (RANS) equations, the RNG  $k - \epsilon$  turbulence model, and the energy equation. The numerical results were in good agreement with experimental data.

Most of the previous work studied the effect of one or more baffles of the same height on heat transfer and pressure drop. The focus was on investigating the Nusselt number and friction factor values, not the difference between the maximum and minimum temperature values. Little research was conducted to numerically deal with fluid flow and heat transfer phenomena in channels with baffles. The objective of the present study is to numerically simulate the fluid flow and heat transfer using sets of different height baffles that are mounted simultaneously on one heater wall in a 2-dimensional rectangular channel. The effects of these sets on the difference between maximum and minimum temperatures of the heater wall as well as Nusselt number, friction factor, and thermal performance enhancement factor as functions of the Reynolds number are to be studied.

## 2. Physical Model

The physical model has a rectangular channel of height,  $H$ , equal to 30 mm, length of 1000 mm, and an infinite width. The entry region is 600 mm, which equals ten times the hydraulic diameter,  $D=60$  mm, to ensure fully developed velocity distribution at the beginning of the test section. The test section has a length,  $L$ , of 400 mm with a 2 mm thickness heater plate beneath it which is made of aluminum and is heated from the bottom. The baffles are mounted on the heater plate at distances of 50 mm, 150 mm, and 250 mm from the upstream edge of the test section, as shown in Figure 1. Three baffles having different heights,  $e$ , of 5 mm, 7.5 mm, and 10 mm each are used. The three baffles are exchanged in order to cover 6 possible cases. There are more three cases where the test section has baffles of the same height. Numbers 1, 2 and 3 refer to baffle heights of 5 mm, 7.5 mm, and 10 mm respectively. These numbers are used to show the order of baffles in the test section from upstream to downstream. For example, the case 1-2-3 indicates that baffle 1 is the upstream baffle, 2 is the middle one while 3 is the downstream baffle as shown in Figure 1. Table 1 shows the 9 different cases. Cases 4 through 9 have an average baffle height equal to that of case 2.

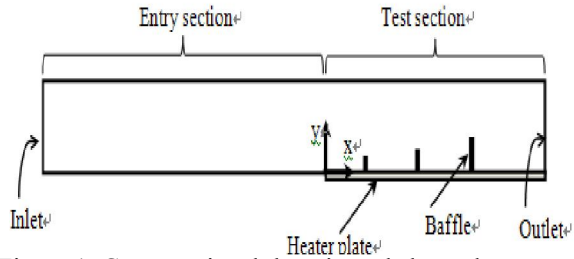


Figure 1. Computational domain and channel geometry of case 1-2-3.

Table 1. Different combinations of baffles used in this study.

Case #	Baffles Order
1	1-1-1
2	2-2-2
3	3-3-3
4	1-2-3
5	1-3-2
6	2-1-3
7	2-3-1
8	3-1-2
9	3-2-1

**3. Mathematical Formulation**

**3.1 Governing equations**

The Reynolds averaged Navier–Stokes (RANS) equations are solved using the k-ε turbulence model and the energy equation. The assumptions of the analysis are steady two-dimensional heat and fluid flows, neglecting body forces and radiation heat transfer, constant properties, and incompressible flow. The governing equations of conservation of mass and momentum are [18]:

$$\frac{\partial}{\partial x_i}(\rho \bar{u}_i) = 0 \tag{1}$$

$$\frac{\partial}{\partial x_j}(\rho \bar{u}_i \bar{u}_j) = \frac{\partial \bar{p}}{\partial x_i} + \frac{\partial}{\partial x_j} \left[ \mu \left( \frac{\partial \bar{u}_i}{\partial x_j} + \frac{\partial \bar{u}_j}{\partial x_i} - \frac{2}{3} \delta_{ij} \frac{\partial \bar{u}_l}{\partial x_l} \right) \right] + \frac{\partial}{\partial x_j}(-\rho \bar{u}_i \bar{u}_j) \tag{2}$$

As the problem under consideration is 2-dimensional, the repeated indices indicate summation from one to two.  $\bar{u}_i$  and  $\bar{u}_i'$  are the mean and fluctuating components of velocity in the direction  $x_i$ .  $\rho$  is mean density,  $\bar{p}$  is mean pressure,  $\mu$  is the molecular viscosity and  $-\rho \bar{u}_i \bar{u}_j$  are the Reynolds stresses. Applying the Boussinesq hypothesis that relates the Reynolds stresses to the mean velocity gradients within the flow, the Reynolds stresses can be evaluated as:

$$-\rho \bar{u}_i \bar{u}_j' = \mu_t \left( \frac{\partial \bar{u}_i}{\partial x_j} + \frac{\partial \bar{u}_j}{\partial x_i} \right) - \frac{2}{3} \delta_{ij} \left( \rho k + \mu_t \frac{\partial \bar{u}_l}{\partial x_l} \right) \tag{3}$$

where  $\mu_t$  is the turbulent viscosity, and  $k$  is the turbulent kinetic energy. The Standard k-ε turbulence model is one of the most common turbulence models that is applied to many engineering flows and provides reasonable accuracy for a wide range of flows. The  $k$  and  $\epsilon$  reflect the energy and scale of turbulence respectively. The k-ε model relates the turbulent viscosity to  $k$  and  $\epsilon$ , such as:

$$\mu_t = \rho C_\mu \frac{k^2}{\epsilon} \tag{4}$$

where  $C_\mu$  is a constant. For steady-state and incompressible flow, the transport equations for  $k$  and  $\epsilon$ , are given by:

$$\frac{\partial}{\partial x_i}(\rho k \bar{u}_i) = \frac{\partial}{\partial x_j} \left[ \left( \mu + \frac{\mu_t}{\sigma_k} \right) \frac{\partial k}{\partial x_j} \right] + G_k - \rho \epsilon \tag{5}$$

$$\frac{\partial}{\partial x_i}(\rho \epsilon \bar{u}_i) = \frac{\partial}{\partial x_j} \left[ \left( \mu + \frac{\mu_t}{\sigma_\epsilon} \right) \frac{\partial \epsilon}{\partial x_j} \right] + C_{1\epsilon} \frac{\epsilon}{k} G_k - C_{2\epsilon} \rho \frac{\epsilon^2}{k} \tag{6}$$

where  $\sigma_k$  and  $\sigma_\epsilon$  are the turbulent Prandtl numbers for  $k$  and  $\epsilon$  respectively and  $C_{1\epsilon}$  and  $C_{2\epsilon}$  are constants.  $G_k$  is the generation of turbulent kinetic energy due to the mean velocity gradients and is approximated according to the Boussinesq hypothesis as:

$$G_k = \mu_t S^2 \tag{7}$$

where  $S$  is the modulus of the mean rate-of-strain tensor, defined by:

$$S = \sqrt{2 S_{ij} S_{ij}} \tag{8}$$

$$S_{ij} = \frac{1}{2} \left( \frac{\partial \bar{u}_i}{\partial x_j} + \frac{\partial \bar{u}_j}{\partial x_i} \right) \tag{9}$$

The constants were evaluated experimentally and their values are:  $C_\mu=0.09$ ,  $\sigma_k = 1.0$ ,  $\sigma_\epsilon = 1.3$ ,  $C_{1\epsilon} = 1.44$ , and  $C_{2\epsilon} = 1.92$ [18].

The energy equation can be written as:

$$\frac{\partial}{\partial x_i}(\rho \bar{u}_i E) = \frac{\partial}{\partial x_j} \left[ K_{eff} \frac{\partial T}{\partial x_j} \right] \tag{10}$$

$E$  is the total energy, and  $K_{eff}$  is the effective thermal conductivity which can be expressed as a function of the thermal conductivity,  $K$ , and the turbulent thermal conductivity,  $K_t$ :

$$K_{eff} = K + K_t \tag{11}$$

$$K_t = C_p \mu_t / Pr_t \tag{12}$$

where  $Pr_t$  is the turbulent Prandtl number.

**3.2 Data reduction**

At steady state condition, the heat flux applied

at the bottom surface of the heater plate,  $q_{bc}$ , is transferred by convection from the upper surface of the heater plate to the fluid,  $q_{conv}$ .

$$q_{conv} = q_{bc} \tag{13}$$

The local heat transfer coefficient,  $h_x$ , can be calculated as:

$$q_{conv} = h_x(T_{p,x} - T_{b,x}) \tag{14}$$

where  $T_{p,x}$  is the local temperature of the upper surface of the heater plate, while  $T_{b,x}$  is the bulk fluid temperature at  $x$ . The bulk fluid temperature can be found from the following relation:

$$q_{conv} x = \dot{m} C_{p,f}(T_{b,x} - T_{b,x=0}) \tag{15}$$

where  $\dot{m}$  is the fluid mass flow rate per unit width. The local Nusselt number can be found as:

$$Nu_x = h_x D / K_f \tag{16}$$

where  $D$  is the hydraulic diameter and  $K_f$  is the thermal conductivity of the fluid. The average Nusselt number is given by:

$$Nu = \frac{1}{L} \int_0^L Nu_x dx \tag{17}$$

where  $L$  is the length of the test section. The friction factor is calculated over the test section length as:

$$f = 2D\Delta p / L\rho u^2 \tag{18}$$

where  $\Delta p$  is the pressure drop over the test section, while  $u$  is the average inlet velocity.

The thermal enhancement factor is the ratio of the heat transfer coefficient of a roughed surface to that of a smooth surface at equal pumping power and can be expressed as:

$$TEF = (Nu/Nu_s)(f_s/f)^{1/3} \tag{19}$$

where  $Nu_s$  and  $f_s$  are the Nusselt number and friction factor of a smooth channel. The  $Nu_s$  for a smooth channel can be expressed by the Dittus-Boelter correlation for heating as [19]:

$$Nu_s = 0.023 Re^{0.8} Pr^{0.4} \tag{20}$$

Also, the friction factor of a smooth channel can be expressed by the Blasius correlation [19]:

$$f_s = 0.316 Re^{-0.25} \tag{21}$$

From a design point of view, it may be good practice not to allow a large difference between the

heater plate maximum and minimum temperatures. The Standard Deviation of heater plate temperature,  $\sigma_T$ , is used as a measuring tool which can be evaluated as follow:

$$\sigma_T = \sqrt{\sum_{i=1}^N (T_{p,x} - \bar{T}_p)^2 / N} \tag{22}$$

where  $T_{p,x}$  and  $N$  are the local temperature value and the number of temperature data points of the upper surface of the heater plate, respectively.  $\bar{T}_p$  is the mean value of temperatures.

#### 4. Results and Discussion

##### 4.1 Verification of the numerical simulations

In order to validate the numerical procedure, turbulence model, and meshing size function, the numerical results of heat transfer and fluid flow are compared with the experimental results of Karwa et al. [3]. Although the experimental physical domain is a 3-dimensional problem, in this study it can be approximated to a 2-dimensional one and the effect of side walls can be neglected as the experimental channel width to height is large, 7.77. Chaube et al. [20] performed 2-D numerical simulations of ribs and compared the numerical results with the experimental data of Karwa [21] where the channel width to height ratio was 7.5. Also, they conducted 2-D and 3-D numerical simulations of the experimental work of Tanda, [22] where the channel width to height ratio was 5. Comparing the 2-D and 3-D numerical models, they concluded that the 2-D results yielded results that are closer to the experimental ones.

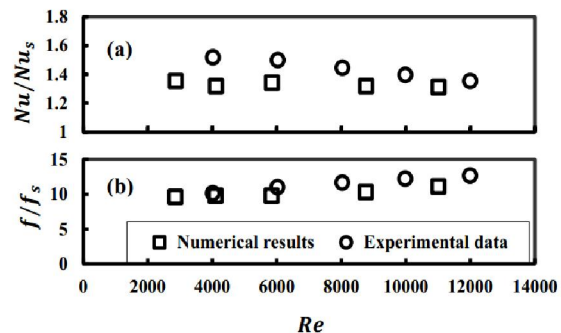


Figure 2. Comparison of the numerical results of the present study and the experimental data of Karwa et al. [3] (a) Nusselt number ratio (b) friction factor ratio.

In the present numerical validation work, the computational test section dimensions are the same as that of the experimental test section of Karwa [3]. The length and height of the computational domain are 1651.8 mm and 38.4 mm respectively. The baffle is made of aluminum while its height is 19 mm and its thickness is 0.9 mm. Two baffles were used in the experimental work with upstream, between, and downstream distances equal to each other with a value

of 550 mm. Mesh is generated with concentrated nodes around baffles using GAMBIT. Computations are performed with the finite-volume-based software FLUENT. Standard  $k-\epsilon$  turbulence model with enhanced wall treatment are applied.

The Nusselt number ratio,  $Nu/Nu_s$ , and friction factor ratio,  $f/f_s$ , versus the Reynolds number of the experimental data and computational results are shown in Figs. 2a and b, respectively. Both of the numerical  $Nu/Nu_s$  and  $f/f_s$  results underestimate the experimental ones. The numerical results are in good agreement with the experimental results.

#### 4.2 Computational domain of the case studies

To study the different cases described in Table 1, the computational domain is assumed to be 2-D as the width of the channel is assumed to be infinite. Mesh is generated with GAMBIT using the same meshing size function used in the previous verification study and concentrated nodes around baffles, as shown in Figure 3. Computations are also performed with the finite-volume-based software FLUENT using the standard  $k-\epsilon$  turbulence model with enhanced wall treatment.

A uniform velocity of air at 300 K is applied at the inlet section while zero pressure is applied at the outlet section. No slip boundary condition is applied at channel and baffle surfaces in contact with fluid. A constant heat flux of  $4,000 \text{ W/m}^2$  is applied at the bottom of the heater plate while an adiabatic condition is applied at the upper surface of the computational domain. The air properties are assumed constant over the computational domain at 300 K. The Reynolds number changes as the inlet air velocity changes.

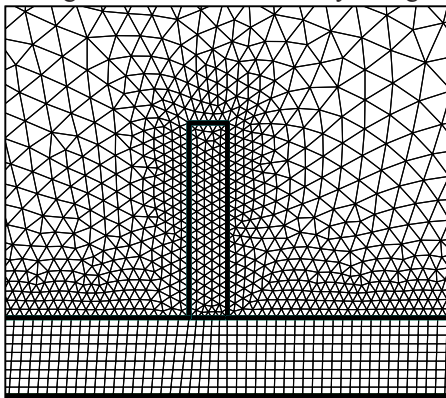


Figure 3. Computational grid around baffle.

#### 4.3 Effect of baffle arrangement on $Nu/Nu_s$

Figure 4 shows the changes of the  $Nu/Nu_s$  as a function of  $Re$  for the 9 cases under consideration. Figure 4a shows a comparison for the three cases where the leading baffle is the shortest, 5 mm. It can be seen that when using 5 mm height for all three baffles, as in cases 1-1-1, the  $Nu/Nu_s$  is at its minimum. This is due to less blockage area in front of the flow, which leads

to less turbulence and less baffle surface area exposed to the flow. The second and third cases, 1-2-3 and 1-3-2, used 7.5 mm and 10 mm for the second and third baffles. The  $Nu/Nu_s$  values are very close for these two cases, but higher than that of case 1-1-1, as the average baffle height is higher, causing more turbulence to occur.

Cases where the leading baffle is at medium height, 7.5 mm, are depicted in Fig. 4b. It is found that when using a height of 7.5 mm for all three baffles, as in case 2-2-2, the  $Nu/Nu_s$  is at its minimum. This indicates that using the same height for all baffles gives less turbulence flow. In general, at each  $Re$  number, the difference between the  $Nu/Nu_s$  values for the three cases is minimal because the average baffle area of exposure is the same and the effect of turbulent eddies is almost identical.

The last three cases that have leading baffles of 10 mm are compared in Figure 4c. Case 3-3-3 has the maximum  $Nu/Nu_s$  compared to the other cases. It has a larger blockage ratio which causes more turbulence. The second and third cases, 3-1-2 and 3-2-1, used 5 mm and 7.5 mm for second and third baffles. Very little difference is found in the  $Nu/Nu_s$  values between the last two cases as the average blockage ratios are the same.

Comparing all cases except the cases 1-1-1 and 3-3-3, Figure 4 shows that there is a slight enhancement of the Nusselt number ratio by up to 3% when the leading baffle is tall. This indicates that causing large eddies upstream enhances flow mixing and heat transfer over the heater plate.

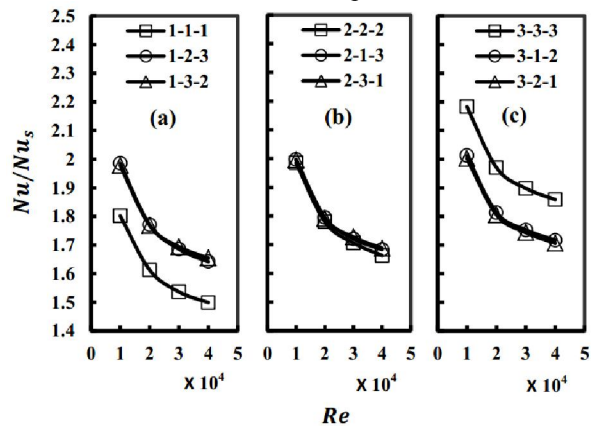


Figure 4. Nusselt number ratio,  $Nu/Nu_s$ , versus  $Re$  for leading baffle heights of (a) 5 mm, (b) 7.5 mm, and (c) 10 mm.

#### 4.4 Effect of baffle arrangement on $f/f_s$

Figure 5 shows the changes of  $f/f_s$  as a function of  $Re$  for the three cases where the leading baffle is the shortest, 5 mm. It can be seen that when using a height of 5 mm for all three baffles,  $f/f_s$  is minimum. This is attributed to the less blockage area in

front of the flow, which means less turbulence. The second and third cases used 7.5 mm and 10 mm for the second and third baffles. A small difference is found between the last two cases. The second group of cases to be compared has a medium leading edge, 7.5 mm. It is clear from Figure 5b that case 2-2-2, which has baffles of equal heights, has less  $f/f_s$  and accordingly it has less turbulence compared to the other two cases. Also, it is indicated that when the middle baffle has the shortest height, case 2-1-3, the  $f/f_s$  has higher values. The same observation is clear in Figure 5c as case 3-1-2 has higher  $f/f_s$  value compared to case 3-2-1. Case 3-3-3 has the highest  $f/f_s$  values as it has the highest baffle blockage ratio.

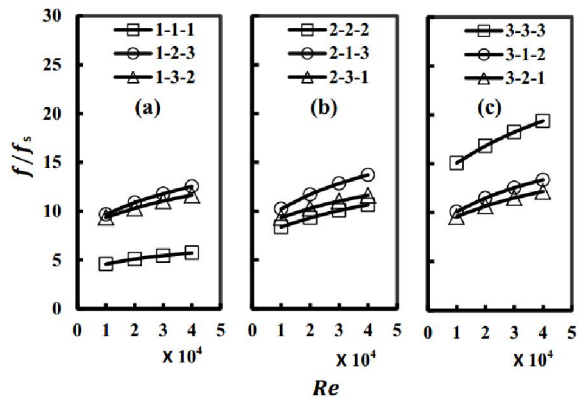


Figure 5. Friction factor ratios,  $f/f_s$ , versus  $Re$  for leading baffle heights of (a) 5 mm, (b) 7.5 mm, and (c) 10 mm.

4.5 Performance evaluation

Standard deviation of temperature

To show the effect of baffle arrangement on temperature distribution of the heater plate upper surface, three cases, 1-2-3, 2-2-2, and 3-2-1 at  $Re=10,000$  are depicted in Figure 6. The differences between the maximum and minimum temperature values are less in case 1-2-3 compared with the other two cases. For case 1-2-3, the shortest baffle is located at the beginning of the test section, raising the temperature of the upstream half of the heater plate compared to the other two cases. Also, for case 1-2-3, the tallest baffle is mounted where the temperature is highest, which reduces the maximum temperature of the downstream half of the heater plate compared with the other two cases. The temperature distribution shows the advantage of using baffles with multiple heights and mounting the tall baffles at places where temperatures are higher than that of other places. It should be noted that case 1-2-3 has almost the same friction factor ratio as that of case 3-2-1 and is close to that of case 2-2-2, as shown in Figure 5. This means that we can have the advantage of decreasing the

maximum temperatures of the heater plate without using additional pumping power.

To measure the difference between the maximum and minimum temperature values for different cases, the standard deviation of temperature,  $\sigma_T$ , can be used as depicted in Figures 7a, b and c. It is clear that  $\sigma_T$  decreases as the Reynolds number increases. Comparing the cases that have baffles of constant heights, cases, 1-1-1, 2-2-2, and 3-3-3, the arrangement 3-3-3 shows lower  $\sigma_T$  than the other two cases which indicates that the taller the baffle, the lower the standard deviation of temperature. For cases with baffles of different heights, when placing the short baffle upstream and the tall baffle downstream,  $\sigma_T$  is low. Case 1-2-3 has the lowest  $\sigma_T$  values while case 3-2-1 has the highest  $\sigma_T$  values. It should be noted that the previous observations are for the heating plate case. The average standard deviation of temperature of case 1-2-3 is 28% less than that of case 2-2-2 and 52% less than that of case 3-2-1.

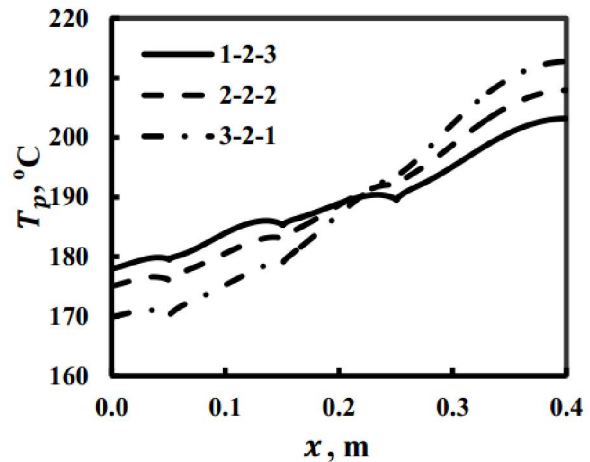


Figure 6. Temperature distributions of heater plate upper surface of three cases at  $Re=10,000$ .

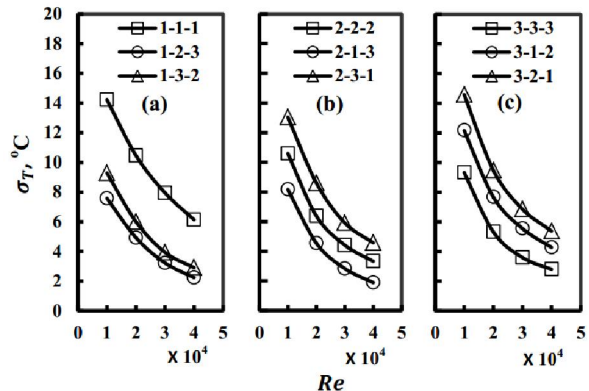


Figure 7. Standard deviation of heater plate temperature.

#### 4.6 Thermal performance enhancement factor

The thermal performance enhancement factor,  $TEF$ , reflects the performance of different case values of  $Nu$  and  $f$  at equal pumping power. Figure 8 shows the  $TEF$  values of different cases. The  $TEF$  decreases as  $Re$  increases for all cases. The best  $TEF$  value is for case 1-1-1, which has the lowest average  $e/H$  value. The lowest  $TEF$  value is for the case that has the highest average  $e/H$  value, case 3-3-3. For the same leading baffle height cases, the  $TEF$  is better when the middle baffle is higher than the downstream one; for example, the  $TEF$  of case 2-3-1 is higher than that of case 2-1-3. Comparing the seven cases of equal average baffle height of  $e/H=0.167$ , the best  $TEF$  value is for case 2-2-2 which has a  $TEF$  value of 6% higher than that of cases 1-2-3. This suggests that from  $TEF$  point of view it is better to use baffles of equal heights.

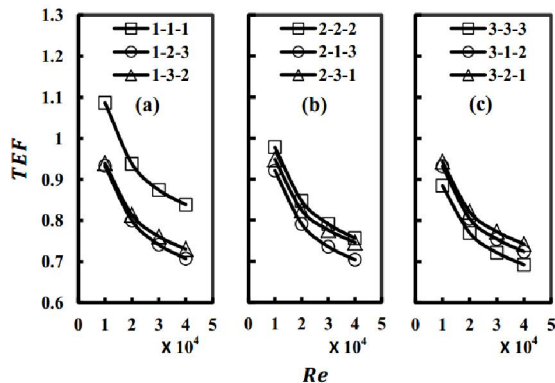


Figure 8. Thermal efficiency factor,  $TEF$ , versus Reynolds number for different cases.

#### 5. Conclusions

A 2-D numerical study has been performed to investigate the effect of baffle height and baffle arrangement on Nusselt number and friction factor ratios for Reynolds number ranges from 10,000 to 40,000. Three baffle to channel height ratios,  $e/H$ , of 0.167, 0.25, and 0.333 are used to form nine different cases. Two different criteria,  $\sigma_T$  and  $TEF$ , are used to measure the performance of baffle arrangements.

All studied cases show that as  $Re$  increases,  $Nu/Nu_s$ ,  $\sigma_T$ , and  $TEF$  decrease and  $f/f_s$  increases. The higher the  $e/H$  value, the higher the  $Nu/Nu_s$  and  $f/f_s$  values. Also, the higher the  $e/H$  value, the lower the  $\sigma_T$  and  $TEF$  values. Comparing the cases that have the same average baffle height indicates that mounting tall baffles in front can enhance  $Nu/Nu_s$  by 3%.

For cases with equal average baffle heights, using baffles of equal height proves to be the best from the  $TEF$  point of view. Using short baffles upstream and tall baffles downstream of the heater plate shows better performance of  $\sigma_T$ , decreasing its value by up to

52%. The maximum heater plate temperature can be decreased without using additional pumping power.

#### Acknowledgement

This work was funded by the Deanship of Scientific Research (DSR), King Abdulaziz University, Jeddah, under grant No. (1431-135-496). The authors, therefore, acknowledge, with thanks, DSR technical and financial support.

#### Corresponding Author:

Dr. Mohamed Hamza  
Mechanical Engineering Department  
Faculty of Engineering at Rabigh  
King Abdulaziz University, Saudi Arabia  
E-mail: [mohamedhamza010@gmail.com](mailto:mohamedhamza010@gmail.com)

#### References

- [1] Habib, M. A., Mobarak, A. M., Sallak, M. A., Hadi, E. A. A., and Affify, R. I., 1994, "Experimental Investigation of Heat Transfer and Flow Over Baffles of Different Heights," *ASME J. Heat Transfer*, 116(2), pp. 363-368.
- [2] Dutta, P., and Hossain, A., 2005, "Internal cooling augmentation in rectangular channel using two inclined baffles," *International Journal of Heat and Fluid Flow*, 26(2), pp. 223-232.
- [3] Karwa, R., Maheshwari, B. K., and Karwa, N., 2005, "Experimental study of heat transfer enhancement in an asymmetrically heated rectangular duct with perforated baffles," *International Communications in Heat and Mass Transfer*, 32(1-2), pp. 275-284.
- [4] Karwa, R., and Maheshwari, B. K., 2009, "Heat transfer and friction in an asymmetrically heated rectangular duct with half and fully perforated baffles at different pitches," *International Communications in Heat and Mass Transfer*, 36(3), pp. 264-268.
- [5] Huang, K. D., Tzeng, S.-C., Jeng, T.-M., Wang, J.-R., Cheng, S.-Y., and Tseng, K.-T., 2008, "Experimental study of fluid flow and heat transfer characteristics in the square channel with a perforation baffle," *International Communications in Heat and Mass Transfer*, 35(9), pp. 1106-1112.
- [6] Lin, C.-W., 2006, "Experimental study of thermal behaviors in a rectangular channel with baffle of pores," *International Communications in Heat and Mass Transfer*, 33(8), pp. 985-992.
- [7] Ko, K.-H., and Anand, N. K., 2003, "Use of porous baffles to enhance heat transfer in a rectangular channel," *International Journal of Heat and Mass Transfer*, 46(22), pp. 4191-4199.
- [8] Promvong, P., 2010, "Heat transfer and pressure drop in a channel with multiple 60° V-baffles," *International Communications in Heat and Mass*

- Transfer, 37(7), pp. 835-840.
- [9] Oh, S. K., Putra, A. B. K., and Ahn, S. W., 2009, "Heat Transfer and Frictional Characteristics in Rectangular Channel with Inclined Perforated Baffles," *World Academy of Science, Engineering and Technology*, 49, pp. 324-329.
- [10] Ary, B. K. P., Lee, M. S., Ahn, S. W., and Lee, D. H., 2012, "The effect of the inclined perforated baffle on heat transfer and flow patterns in the channel," *International Communications in Heat and Mass Transfer*, 39(10), pp. 1578-1583.
- [11] Kwankaomeng, S., and Promvonge, P., 2010, "Numerical prediction on laminar heat transfer in square duct with 30° angled baffle on one wall," *International Communications in Heat and Mass Transfer*, 37(7), pp. 857-866.
- [12] Promvonge, P., Jedsadaratanachai, W., and Kwankaomeng, S., 2010, "Numerical study of laminar flow and heat transfer in square channel with 30° inline angled baffle turbulators," *Applied Thermal Engineering*, 30(11-12), pp. 1292-1303.
- [13] Jedsadaratanachai, W., Suwannapan, S., and Promvonge, P., 2011, "Numerical Study of Laminar Heat Transfer in Baffled Square Channel with Various Pitches," *Energy Procedia*, 9, pp. 630-642.
- [14] Promvonge, P., Sripattanapipat, S., and Kwankaomeng, S., 2010, "Laminar periodic flow and heat transfer in square channel with 45° inline baffles on two opposite walls," *International Journal of Thermal Sciences*, 49(6), pp. 963-975.
- [15] Promvonge, P., Sripattanapipat, S., Tamna, S., Kwankaomeng, S., and Thianpong, C., 2010, "Numerical investigation of laminar heat transfer in a square channel with 45° inclined baffles," *International Communications in Heat and Mass Transfer*, 37(2), pp. 170-177.
- [16] Promvonge, P., and Kwankaomeng, S., 2010, "Periodic laminar flow and heat transfer in a channel with 45° staggered V-baffles," *International Communications in Heat and Mass Transfer*, 37(7), pp. 841-849.
- [17] Sriromreun, P., Thianpong, C., and Promvonge, P., 2012, "Experimental and numerical study on heat transfer enhancement in a channel with Z-shaped baffles," *International Communications in Heat and Mass Transfer*, 39(7), pp. 945-952.
- [18] ANSYS-FLUENT-12.0, 2009, "Theory Guide."
- [19] Incropera, F., and Dewitt, P. D., 2006, "Introduction to Heat Transfer," John Wiley & Sons Inc., Fifth edition.
- [20] Chaube, A., Sahoo, P. K., and Solanki, S. C., 2006, "Analysis of heat transfer augmentation and flow characteristics due to rib roughness over absorber plate of a solar air heater," *Renewable Energy*, 31(3), pp. 317-331.
- [21] Karwa, R., 2003, "Experimental Studies of Augmented Heat Transfer and Friction in Asymmetrically Heated Rectangular Ducts with Ribs on the Heated Wall in Transverse, Inclined, V-Continuous and V-Discrete Pattern," *International Communications in Heat and Mass Transfer*, 30(2), pp. 241-250.
- [22] Tanda, G., 2004, "Heat transfer in rectangular channels with transverse and V-shaped broken ribs," *International Journal of Heat and Mass Transfer*, 47(2), pp. 229-243.

15/5/2013